

Structural Optimization of Dental Restorations using the Principle of Adaptive Growth

Guillaume Couegnat
Ecole des Mines D'Albi,
Carmaux, France

Jonathan E. Cooper
School of Engineering,
University of Manchester, UK

Siu L. Fok
School of Engineering,
University of Manchester, UK

Alison J.E. Qualtrough
Turner Dental School,
University of Manchester, UK

ABSTRACT

Fracture of restored teeth is a problem in restorative dentistry since it has been estimated that 92 percent of fractured teeth have been previously restored. In a restored tooth, the stresses that occur at the tooth-restoration interface during loading could become large enough to fracture the tooth and/or restoration. The tooth preparation process for a dental restoration is therefore a classical optimization problem: tooth reduction must be minimized to preserve tooth tissue whilst stress levels must be kept low to avoid fracture of the restored tooth. The objective of the present study was to propose alternative optimized designs for a second upper premolar cavity preparation by means of structural shape optimization based on the finite element method and biological adaptive growth. Restored tooth models using the optimized cavity shapes exhibited significant reduction of stresses along the tooth-restoration interface. In the best case, the maximum stress value was reduced by more than 50 percent.

Keywords: Structural optimization, dental restorations, adaptive growth, finite element

INTRODUCTION

The anatomy and occlusal relationships of posterior teeth suggest a tendency for the cusps to deflect under stress. While sound teeth can withstand masticatory forces and rarely fracture, cusp fracture could occur in a tooth that has been weakened by caries and cavity preparation. Both clinical and experimental data shows that the fracture resistance of restored teeth is significantly lower than in healthy teeth, regardless of the restorative material. Deep and/or wide restorations pose the greatest risk of tooth fracture. A survey carried out in 1987 found that 92 percent of fractured teeth had been previously restored [1]. Furthermore, even if fracture does not occur, deflection of a weakened cusp may open the tooth-restoration interface and lead to subsequent microleakage resulting in recurrent caries, predisposing the tooth to possible fracture.

A previous project carried out by a student [2] concluded that there are high stress concentration areas at the internal line

angles of the cavity when restorations are not bonded to the tooth and at the dentin-enamel junction for bonded restorations (see Fig. 1). The stress concentration factor was found to reach values as high as 4 or 5. Therefore, it was concluded that fatigue failure could occur as a result of the mastication cycle process, as the degree of stresses in these areas was sufficient to initiate crack propagation.

These results support those obtained by previous studies [3], viz. teeth restored with restorations that are not bonded to the tooth are most likely to fracture at the internal line angles of the cavity due to crack propagation, whilst cracks within teeth containing bonded restorations are most likely to originate within the enamel at the site of occlusal contact with the opposing tooth.

The objective of the present study was to propose, by the means of a method of structural shape optimization based on biological growth, an optimized design for a second upper premolar cavity preparation. The structural shape optimization method was simulated using the finite elements packages MSC/PATRAN and ABAQUS.

Three models of cavity preparations were investigated: a conventional design for preparation of a premolar tooth, an 'undercut' cavity design and a conventional onlay preparation. Three restorative materials and several tooth/restoration contact conditions were utilized to replicate the real conditions as close as possible. The optimization process was run for each cavity geometry.

OPTIMIZATION USING FINITE ELEMENTS AND ADAPTIVE GROWTH

The method used is that based on biological adaptive growth developed and pioneered by Claus Mattheck at the Karlsruhe Research Centre [4]. In simple terms, adaptive growth can be defined as follows:

- Build-up of material at overloaded zones

- No build-up or even reduction of material at underloaded zones

The method can easily be implemented into a finite element (FE) based computational environment; in this case, PATRAN and ABAQUS. The steps are:

1. Create a finite element model corresponding to the first draft for the desired shape of the component. This initial FE model should have a layer of elements of roughly equal thickness on the surface where later growth is to occur (see Fig. 2).
2. Perform a FE computation with the expected operational loading and support to obtain the nodal stresses. These could be the maximum principal stress or the von Mises stress etc., the choice of which would depend on the failure criteria appropriate to the material under consideration.
3. Convert the computed stress to a fictitious temperature. As a result, the sites having the highest mechanical stresses are also the hottest places in the component.
4. In a further FEM computation, only the thermal stress due to the fictitious temperature field is considered, the previous mechanical load being ignored. A reference temperature can be used here to represent the required stress level. Moreover, the modulus of elasticity in the growth layer is reduced to an arbitrarily low value and only this soft upper layer will have a coefficient of thermal expansion $\alpha > 0$, so that the material under it cannot expand thermally. Zones which have the highest load/temperature expand the most. The small Young's modulus prevents jamming of neighboring elements, allowing them to grow compatibly outwards in a direction approximately perpendicular to the surface.
5. Update the nodal coordinates of the model using the displaced geometry. The structure should now have an improved shape. Steps 2-5 are run through repeatedly, until the stresses in the growth area converge to the required level.

APPLICATION TO TOOTH PREPARATION

The investigation was conducted for a second upper premolar using a 2D FE model. The bucco-lingual section of the tooth was the area under analysis since this section is where the higher stresses occur and has been shown to represent the tooth accurately. Only the anatomical crown was investigated, i.e. the tooth was only modeled to a depth of 1 mm into the gingival crevice and the base of the crown was rigidly fixed. The stress distribution in the area of interest was considered not to be affected significantly by the absence of the root.

The geometry of the crown was taken from Wheeler's Atlas [5]. The data on the thickness of enamel and dentin was obtained from measurements reported by Shillingburg [6]. Three cavity designs (Fig. 3) have been considered in this investigation:

- The conventional inlay design (non-undercut) used for indirect with composite or porcelain restorations that are bonded to the tooth, with the vertical walls being

tapered towards the base by 0.3 mm over the length of the tooth.

- The undercut design is an example of tooth preparation generally used with non-bonded restorations, such as amalgam. The undercut allows the restoration to be mechanically locked within the cavity during mastication. The width of the restoration at the cusp was similar to that of the inlay design, however the line angle was altered to widen, instead of narrow, by 0.3 mm over the length of the tooth.
- The onlay cavity design was adapted from the work of Deligeorgi [7], with a conventional cusp reduction of 2.0 mm.

Three restorative materials were used in this study: dental amalgam, composite and porcelain. They were all assumed to be homogeneous and isotropic. Their main mechanical properties are shown in Table 3. Concerning the tooth materials, both enamel and dentin are known to be anisotropic. However, due to the lack of reliable information on the properties of these materials, they were assumed to be isotropic for simplicity, as adopted by most previous investigators.

The models were meshed using 8-noded quadrilateral (QUAD8) elements; see Fig. 4. A convergence study was first carried out, which revealed that convergence was achieved when using elements smaller than 0.5 mm in length. Thus, all meshing were done using approximately 0.3-mm long elements.

The boundary conditions were specified to be consistent with the physiological conditions. Vertical displacements along the base of the model were restricted to simulate support from the alveolar socket (Fig. 5). Horizontal displacements at the base were also fixed to remove rigid body motions. Although the periodontal ligament allows slight movement in the alveolar socket, the above simplification in the boundary conditions should not have a significant effect on the stresses located at the points of interest, i.e. the tooth-restoration interface.

Only static loading was considered. The occlusal load of a typical magnitude was resolved into two oblique components acting perpendicularly to the cuspal inclines which were lying approximately at 45° to the vertical. Contact conditions were created along the tooth-restoration interface to allow for imperfect contact. Several frictional coefficients (μ) were used to simulate the different bonding conditions: 'tied' signified perfect bonding conditions, $\mu=0.5$ represented a deteriorated bond and $\mu=0.01$ was used for virtually no bonding at all between the tooth and the restoration. In total, 27 models were created (3 cavity geometries \times 3 restoration materials \times 3 contact conditions).

Initially, simple FE analysis was performed for each model in order to obtain an overview of the stress pattern within the restored teeth with different cavity preparations and tooth-restoration interfacial conditions. As expected, the analysis revealed some high stress areas along the interface between the tooth and the restoration: at the corners of the cavity for non-bonded restorations and at the dentin-enamel junction for bonded restorations, as depicted in Fig. 6. These findings

confirm the results obtained by previous investigators. However, it should be pointed out that, for both non-undercut and undercut geometries the highest stress values are located within the tooth, whereas for the onlay, they are within the restorations.

These preliminary results also revealed that the highest stress values along the interface occurred when composite was used as the restoration material and there was little or no bonding between the tooth and restoration (i.e. $\mu=0.01$) for all three cavity designs. Therefore, to minimize the amount of computation, it was decided to carry out the optimization using these conditions (composite restoration and $\mu=0.01$) only, since they represented the worst case scenario. It was postulated that using the optimized geometries obtained with these conditions would also decrease the stress values in the other cases, i.e. if the stress values were reduced in the worst case, it could be expected that the same would occur for the other cases. The validity of this assumption would then be checked by applying the optimized shape thus obtained to the other scenarios.

For the purpose of illustration, the reference stress was set arbitrarily at 150 MPa.

NUMERICAL RESULTS & DISCUSSION

For the conventional inlay design, the geometry of the cavity was only slightly altered: the overall curvature of the bottom was increased, as depicted in Fig. 7, while the line angle of the vertical edges remained the same. This slight modification of the geometry appeared to be sufficient to remove the high stresses at the bottom corners. The effect is more obvious when the von Mises stress along the tooth-restoration interface is plotted, as in Fig. 8. The stress peaks are clearly removed, with the maximum von Mises stress value being reduced by about 52 percent. Moreover, the stresses are almost uniform along the interface and they converge to the reference value as expected.

When the other restoration materials were used, instead of composite, with this optimized shape and μ still had the value of 0.01, the results were similar, with a stress reduction of 46 and 47 percent respectively for amalgam and porcelain. Increasing the coefficient of friction to 0.5 produced similar results, but the stress reduction was less (around 35 percent).

With perfect contact between the tooth and restoration, the 'optimized' geometry obtained from considering the worst case scenario did not modify the stress values along the interface (see Fig. 9). This is perhaps not surprising since the highest stress in this case occurs at the enamel-dentin junction where the shape has not been changed. This means that the worst case scenario does not apply in this case and optimization has to be performed explicitly using the correct interfacial conditions. This also raises the question as to whether further reduction in the stress levels could be obtained for the intermediate bonding condition, $\mu=0.5$, if optimization was performed explicitly.

The results for the undercut cavity were very similar to the ones for the conventional design. Whilst the line angle was not modified, the radius of curvature at the bottom of the cavity

was increased to produce a smoother curve between the bottom and vertical edges of the cavity (Fig. 10). Von Mises stresses along the tooth-restoration interface are again very similar to those obtained for the conventional design, with a clear peak reduction and an almost uniform stress distribution approaching the reference value (Fig. 11). Again, the stress reduction was around 50 percent (composite: 52%, amalgam: 48%, porcelain: 49%) for $\mu=0.01$ and around 40-45 percent for $\mu=0.5$. As previously, the stress pattern was not modified significantly when perfect contact was considered.

The results for the onlay restoration were rather different since the highest stress values occurred within the restoration itself (Fig. 12); the unrealistically high stresses at the points of loading were ignored. Hence, the growth layer was located within the restoration rather than within the teeth during the optimization process. The optimized shape has the two lower inner surfaces, originally horizontal, lying at an angle so that they became more perpendicular to the loads; see Fig. 12. Once again, the stress reduction was around 50 percent for $\mu=0.01$ (Fig. 13), 40 percent for $\mu=0.5$ regardless of the restoration material, whereas the stress distribution remained unchanged when perfect contact was considered.

CONCLUSIONS

The shape optimization technique based on biological adaptive growth process has been successfully applied to the tooth reduction procedures in dental restoration. Significant reduction in the stress levels at the tooth-restoration interface where bonding is imperfect has been achieved using the optimized cavity or restoration shapes.

REFERENCES

- [1] Craig, R., 1993, Restorative Dental Materials, 9th edition, pp. 473-490.
- [2] Thompson, S., 2002, Investigation into the magnitude and placement of the stress at the tooth-restoration interface using finite element analysis, MEng thesis, Manchester School of Engineering, University of Manchester.
- [3] Arola, D., Galles, L.A. and Sarubin, M.F., 2001, A comparison of mechanical behaviour of posterior teeth with amalgam and composite MOD restorations, *J. of Dentistry*, **29**, pp. 63-73.
- [4] Mattheck, C. and Burkhardt, S., 1990, A new method of structural shape optimization based on biological growth, *Int. J. Fatigue*, **12**, pp. 185-190.
- [5] Wheeler, R.C., 1969, An Atlas of Tooth Form, 4th edition, London, WB Saunders Company.
- [6] Shillenburg, H.T., Jacobi, R. and Brackett, S.E., 1991, Fundamentals of tooth preparation for cast metal and porcelain restorations, Chicago, Quintessence Publishing Company, pp. 205-258.
- [7] Deligeorgi, V., 2002, Aspects of management in the restoration of molar teeth, PhD thesis, Faculty of Medicine, Dentistry, Nursing and Pharmacy, University of Manchester.

Bucco-lingual max. diameter		9.0 mm
Bucco-lingual diameter at gum line		8.0 mm
Intercuspal distance		5.0 mm
Min. height of crown (at centre)		6.2 mm
Length of crown	Buccal	8.5 mm
	Lingual	8.0 mm
Peak thickness of enamel at top	Buccal	1.7 mm
	Lingual	1.7 mm
Thickness of enamel at peak diameter	Buccal	1.3 mm
	Lingual	1.4 mm
Thickness of dentin at peak diameter	Buccal	3.3 mm
	Lingual	3.4 mm
Thickness of dentin at gum line	Buccal	2.2 mm
	Lingual	2.3 mm

Table 1 Typical dimensions of a second premolar

Type of restoration	Width at top	Width at base	Depth at centre	Depth at buccal cusp	Depth at lingual cusp
Conventional	3.5 mm	3.2 mm	1.5 mm	3.8 mm	3.6 mm
With undercut	3.5 mm	3.8 mm	1.5 mm	3.8 mm	3.6 mm

Table 2 Dimensions of inlay restorations with and without undercut [2]

	Young's Modulus	Poisson's ratio	Compressive strength	Tensile strength	Shear strength
Composite	19 GPa	0.24	277 MPa	45 MPa	122 MPa
Amalgam	50 GPa	0.29	388 MPa	50 MPa	188 MPa
Porcelain	69 GPa	0.25	172 MPa	110 MPa	34 MPa
Enamel	80 GPa	0.30	384 MPa	10.3 MPa	90 MPa
Dentin	20 GPa	0.31	297 MPa	98.7 MPa	138 MPa
Pulp	2.07 MPa	0.45	N/A	N/A	N/A

Table 3 Properties of restoration and tooth materials

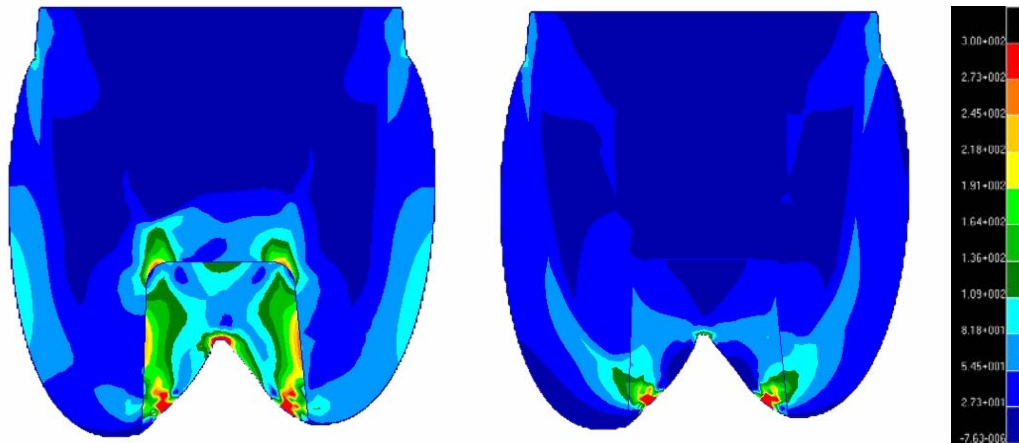


Figure 1 Von Mises stress (MPa) pattern in a restored tooth (left: not bonded, right: bonded)

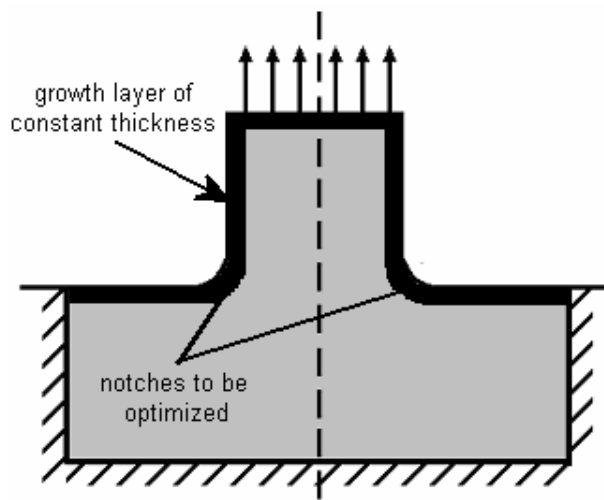


Figure 2 Example of growth layer on a tension plate with narrowing cross-section

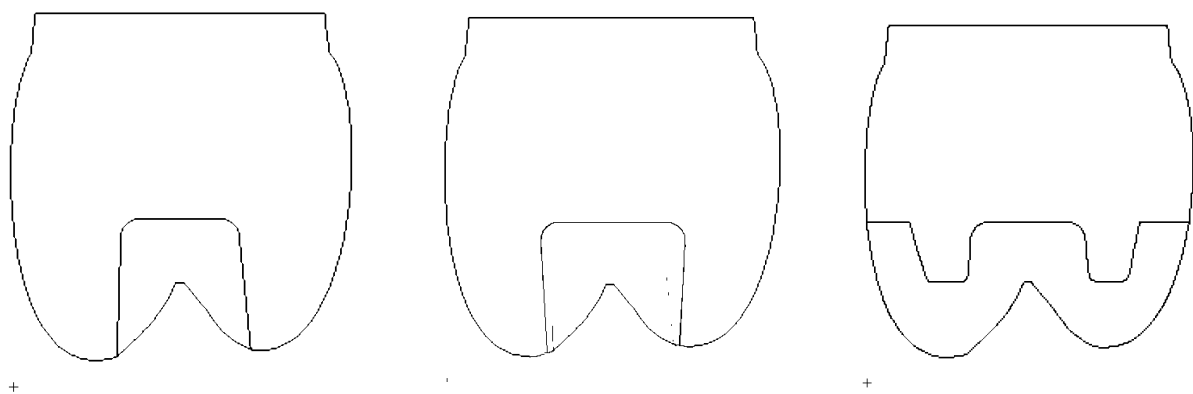


Figure 3 Cavity preparation designs: conventional inlay, undercut and onlay

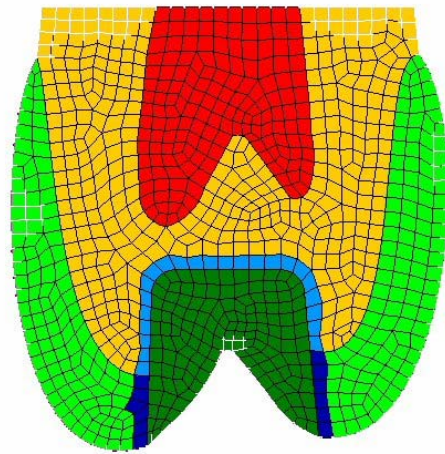


Figure 4 Materials: pulp (red), dentin (yellow), enamel (light green), filling material (dark green) and growth layer (blue)

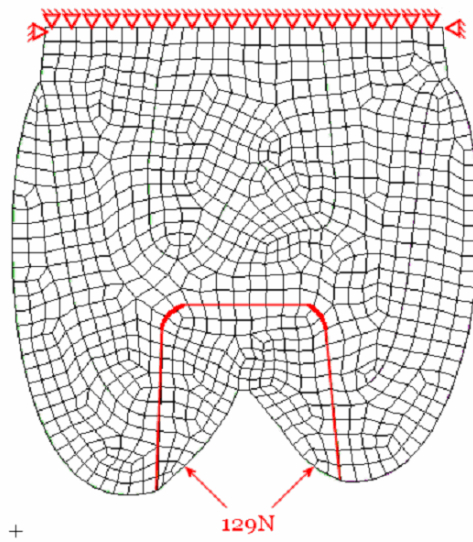


Figure 5 Boundary and loading conditions of the model

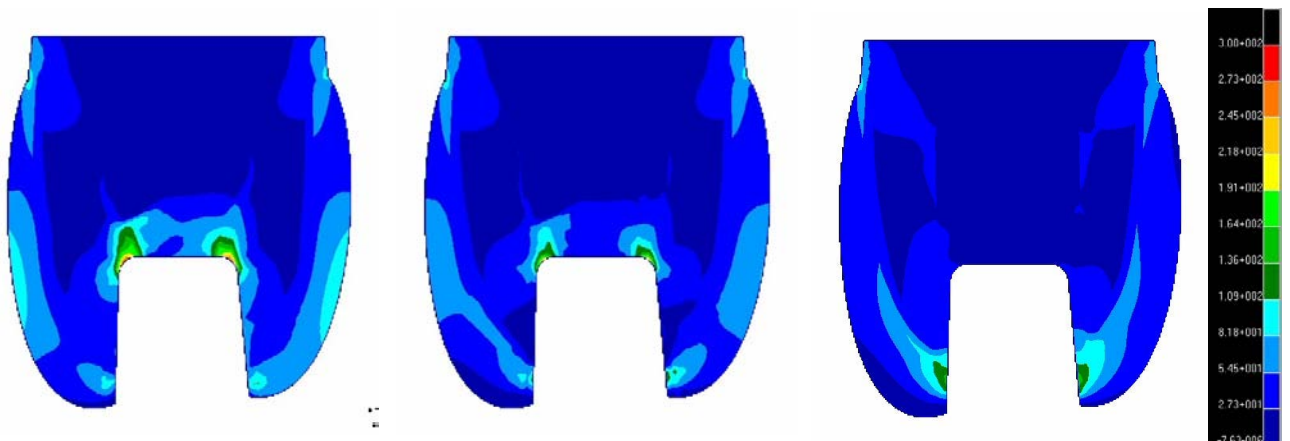


Figure 6 Von Mises stress (MPa) pattern for the conventional cavity design with amalgam as restoration material ($\mu=0.01$, $\mu=0.5$, tied)

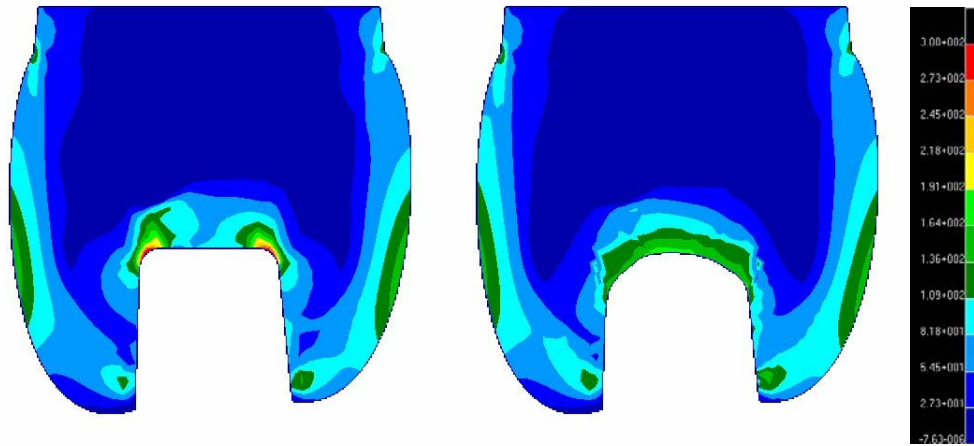


Figure 7 Von Mises stress (MPa) pattern for the conventional inlay cavity with composite restoration and $\mu=0.01$ (left: original, right: optimized)

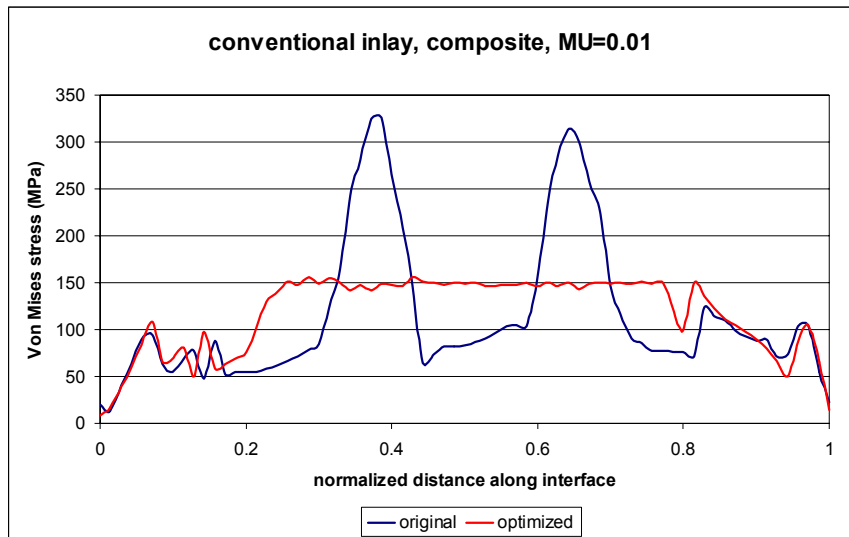


Figure 8 Von Mises stress along tooth-restoration interface for conventional inlay with composite restoration and $\mu=0.01$

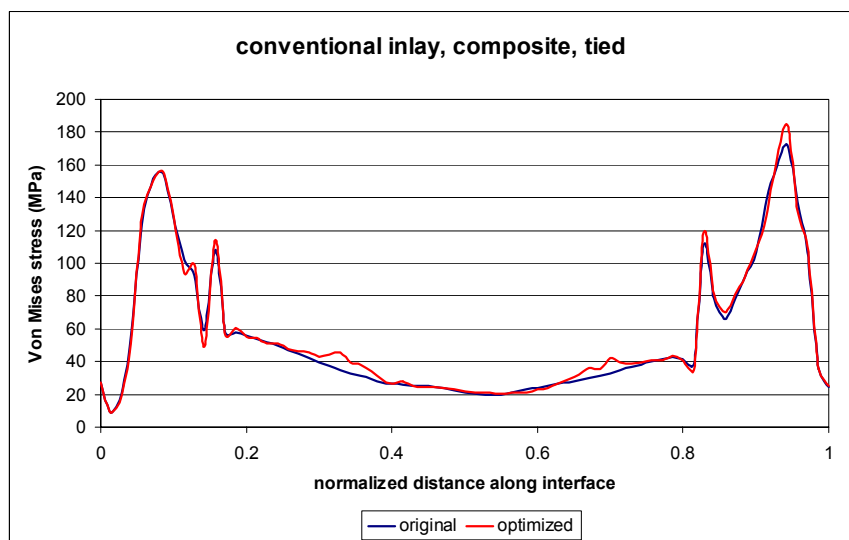


Figure 9 Von Mises stress along the interface for the conventional inlay cavity, composite restoration, tied

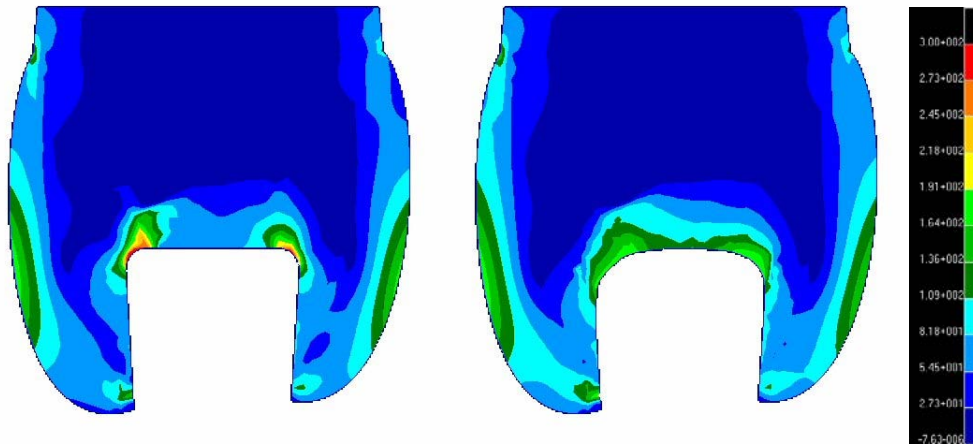


Figure 10 Von Mises stress (MPa) pattern for the undercut cavity, composite restoration and $\mu=0.01$ (left: original, right: optimized)

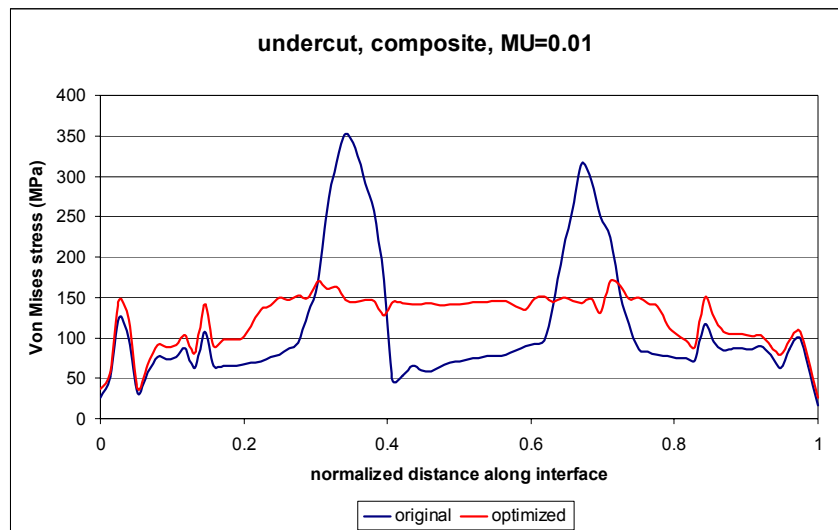


Figure 11 Von Mises stress distribution along tooth-restoration interface for inlay with undercut, composite restoration and $\mu=0.01$

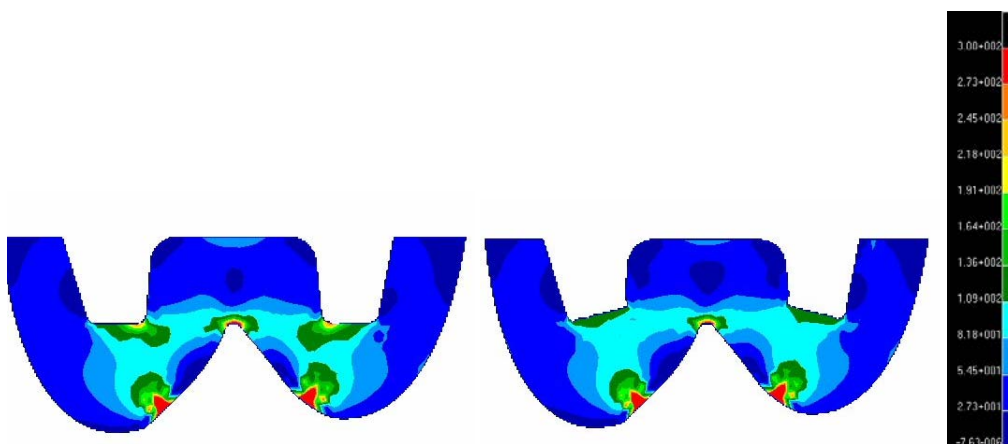


Figure 12 Von Mises stress (MPa) pattern for the onlay restoration with composite and $\mu=0.01$ (left: original, right: optimized)

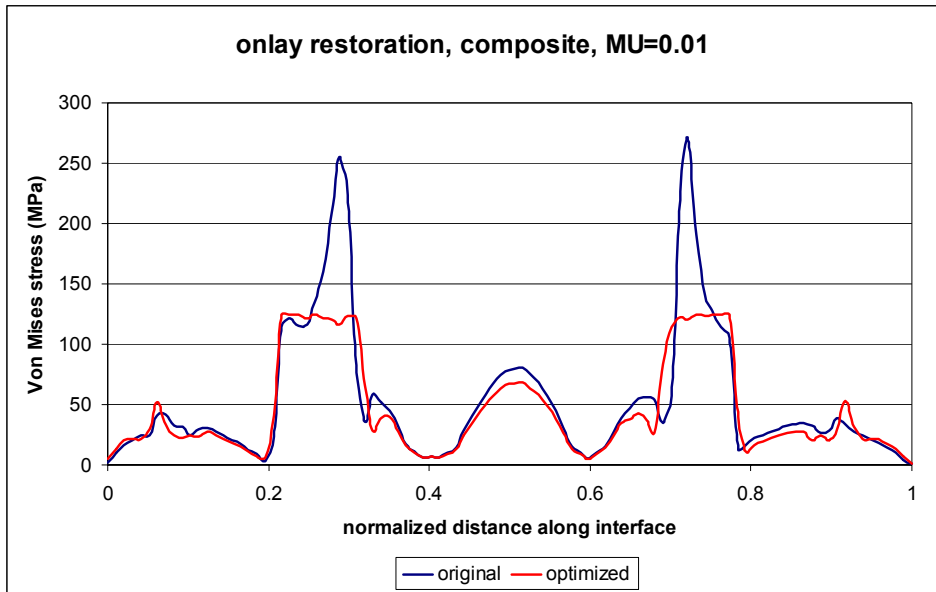


Figure 13 Von Mises stress along tooth-restoration interface for onlay restoration with composite and $\mu=0.01$